Noise and the PSTH response to current transients: I. General theory and application to the integrate-and-fire neuron.

A. Herrmann (alix.herrmann@epfl.ch) † and W. Gerstner (wulfram.gerstner@epfl.ch)
Centre for Neuro-Mimetic Systems
Swiss Federal Institute of Technology, Lausanne
CH-1015 Lausanne-EPFL, Switzerland

Abstract. An analytical model is proposed that can predict the shape of the post-stimulus time histogram (PSTH) response to a current pulse of a neuron subjected to uncorrelated background input. The model is based on an explicit description of noise in the form of an escape rate and corresponding hazard function. Two forms of the model are presented. The full model is nonlinear and can be integrated numerically while a linearized version, while the linearized version can be solved analytically. In the linearized version, the PSTH response to a current input is proportional to a filtered version of the input pulse. The bandwidth of the filter is determined by the amount of noise. In the limit of high noise, the response is similar to the time course of the potential caused by the input pulse, while for low noise it is proportional to its derivative. For low noise, a second peak occurs after one mean interval. The full nonlinear model predicts an asymmetry between excitatory and inhibitory current inputs. We compare our results with simulations of the integrate-and-fire model with stochastic background input. We predict that changes in PSTH shape due to noise should be observable in many types of neurons in both subthreshold and suprathreshold regimes.

Keywords: PSTH, noise, integrate-and-fire, noisy integration

1. Introduction

How are temporal signals transmitted by neurons in the presence of noisy background input? In particular, what is the typical response of a neuron to a single presynaptic spike? To answer this question, one experimental approach has been to study the temporal response of the a single neuron to an input current pulse that mimics the time course of a postsynaptic current elicited by an incoming spike (Fetz and Gustafsson, 1983; Poliakov et al., 1996). Those studies clearly established that background noise has an influence on the response in tonically firing (suprathreshold) neurons. However, the exact nature of this influence is not yet fully understood.

† Corresponding author. Tel: ++41 21 693 3910, Fax: ++41 21 693 5263

In this paper we present a theoretical approach describing the effect of noise on the response of a spiking neuron that incorporates 1) an explicit noise model and 2) a postsynaptic potential (PSP) of arbitrary shape and the membrane potential trajectory following a spike, including the afterhyperpolarization potential (AHP). We then use the model to predict the responses of an integrate-and-fire type neuron model with different levels of diffusion noise. In the companion paper (Herrmann and Gerstner, 2000) we use a slightly more realistic spiking neuron model with parameters adapted to motoneurons in order to compare our theoretical predictions with published experimental data from motoneurons.

Experimentally, a neuron's response to an input spike generating a postsynaptic potential pulse is measured with the peristimulus time histogram (PSTH), i.e. the probability of firing as a function of time t since the stimulus, here denoted $PSTH(t)$. Physiologists have long suspected that the shape of the PSTH response to a pulse is determined by the amount of synaptic noise, the time course of the postsynaptic potential (PSP), and its derivative (Moore et al., 1970; Knox, 1974; Kirkwood and Sears, 1978; Fetz and Gustafsson, 1983; Poliakov et al., 1997); see also (Abeles, 1991). The basic scenario is illustrated in Fig. 1. The experimental record documenting the effect of noise from stochastic background synaptic activity on the PSTH response ranges from *Aplysia* to motoneurons in cat, and we believe the underlying principles are even more generally applicable. Briefly, theoretical analyses have been made for two cases: a neuron in the subthreshold regime subjected to substantial noise, and a noiseless neuron in the suprathreshold regime. By making simplifying assumptions, the theories proposed were able to qualitatively account for the observed changes in the PSTH, but do not fully explain the experimental record (Poliakov et al., 1996; Poliakov et al., 1997) or allow the PSTH to be predicted for a given noise level. In the companion article we will give an extensive overview of that debate. Here we simply state that this question is still open in the experimental literature. In this article, we develop a rather general theoretical framework to answer this question. We illustrate the approach with the standard integrate-and-fire neuron. Because of its single time constant, an integrate-and-fire model can can only capture a limited range of the behavior of a real neuron. In the companion article we will apply our theoretical results to a slightly more detailed spiking neuron model in order to compare our results with published experimental data.

Briefly, our approach may be summarized in the following three steps. First, noise due to stochastic background activity is modeled as diffusion noise (Stein, 1967). In neurons with diffusion noise, the noise level appears to control the relative influence of the PSP and its derivative on the shape of the PSTH profile in the same way as in the (suprathreshold) motoneuron experiments. As a reference model, we study the integrate-and-fire model. Second, in order to avoid the mathematical difficulties of diffusion noise, we replace it by escape-rate noise (Plesser and Gerstner, 2000). We identify an escape rate function that gives a good match to diffusion noise over a wide range of mean inputs and demonstrate how it can be used to predict the PSTH. Finally, using a linearized version of the full model we show analytically how the noise level controls the response.

Fig. 1 gives an overview. For $t < 0$, a neuron is subjected to diffusion noise superimposed on a constant current. It fires randomly with a mean level of activity given by A_0 (spikes/sec); the mean interspike interval is the inverse of the mean firing rate, i.e. $T_0 = 1/A_0$. At time $t = 0$, a current pulse $I(t)$ is applied. The resulting postsynaptic potential $PSP(t)$ may or may not drive the neuron to threshold, causing a spike to be fired. Repetition of this process yields the PSTH, an estimate of the probability $PSTH(t)$ of an extra spike following the pulse.

The size and shape of the PSTH depend on the noise level. Increasing the noise amplitude increases the baseline firing rate and decreases the amplitude of the PSTH peak. For high noise, the function $PSTH(t)$ appears approximately proportional to $PSP(t)$; cf. Fig. 1, right column. For low noise, $PSTH(t)$ is reminiscent of the PSP derivative, $PSP'(t)$, which features a trough following the peak; however, the time courses of $PSP'(t)$ and $PSTH(t)$ are frequently different (Poliakov et al., 1996). This effect of noise on the time course of the PSTH is what we will try to explain with a theory.

2. Methods

In this section, we begin by defining a general, deterministic neuron model, the spike-response model. We then define a noise model based on escape rates which allows us to calculate the interval distribution and survivor function. In Sec. 3 we will apply these functions to obtain a theory predicting the PSTH of a single neuron responding to a small pulse; to illustrate our findings, we will apply the theory to integrate-and-fire neurons with diffusion noise and compare our theoretical predictions to simulations.

2.1. Neuron model: The spike-response model

The spike-response model (Gerstner, 1995; Gerstner, 1999; Gerstner, 2000) consists of a threshold ϑ, a refractory function η, and a response kernel ε describing the response of the neuron to an external current input $I(t)$.

The refractory function $\eta(t-\hat{t})$ generates the afterhyperpotential following a spike at time $\hat{t}$ (Fig. 2). The kernel $\varepsilon(t-\hat{t},s)$ describes the response of the membrane to a small fluctuation at $s=0$; the $t-\hat{t}$ dependence allows spike-dependent conductance changes to be represented. The net input potential

$$h(t|\hat{t}) = \int_0^\infty \varepsilon(t-\hat{t},s) I(t-s) ds \tag{1}$$

integrates the current input $I(t)$. The resulting membrane potential $u(t)$ is the sum of the (negative) refractory potential and the net input potential,

$$u(t) = \eta(t-\hat{t}) + h(t|\hat{t}) \tag{2}$$

where $\hat{t}$ is the last firing time of the neuron. When the membrane potential exceeds the threshold, a spike is emitted and the potential is reset by setting $\hat{t}=t$ in Eq. 2. With an appropriate choice of the kernels ε and η, the spike-response model can reproduce the dynamics of the Hodgkin-Huxley model to a high degree of accuracy (Kistler et al., 1997).

The following exponential kernels result in a neuron equivalent to the standard integrate-and-fire model (Gerstner, 1995; Gerstner, 2000):

$$\eta(t-\hat{t}) = -\eta_0 e^{-\frac{(t-\hat{t})}{\tau_{\rm m}}} H(t-\hat{t}) \tag{3}$$

$$\varepsilon(t-\hat{t},s) = \frac{R}{\tau_{\rm m}} e^{-\frac{s}{\tau_{\rm m}}} H(s) H(t-\hat{t}-s) \tag{4}$$

where $\tau_{\rm m}$ is the membrane time constant, R is the input resistance, η_0 is a scale factor for the refractory function, and $H(\cdot)$ is the Heaviside step function with $H(x)=0$ for $x \le 0$ and $H(x)=1$ for $x>0$. The membrane time constant $\tau_{\rm m}$ and input resistance R would be determined experimentally from the response to small currents. With this choice of kernels the deterministic membrane potential evolves between spikes according to the standard integrate-and-fire equation:

$$-\tau_{\rm m} \frac{d}{dt} u(t) = u(t) + RI(t) \tag{5}$$

Following a spike the membrane potential is reset to $u(\hat{t}) = -\eta_0$. For constant input I_0, the input potential is $h_0(t|\hat{t}) = RI_0(1-\exp[-(t-$

$\hat{t})/\tau_m]$); in this paper, we sometimes write h_0 (with no arguments), meaning $h_0 = h_0(t, -\infty) = RI_0$.

Although in this paper we use the above simple, exponential kernels for the purpose of illustration, we emphasize that the spike-response model is more general because in principle the refractory and PSP kernels η and ε can take any form desired and can for example accomodate an absolute refractory period or synaptic delay, or be fit to more realistic models (Kistler et al., 1997). The model does not include effects arising from adaptation, which we exclude in order to study neuronal behavior close to a steady state.

2.2. Noise models

Taken by itself, the spike-response model is completely deterministic. Now we investigate the effect of adding noise. Our starting point is diffusion noise, motivated by stochastic spike arrival (Stein, 1967). For the standard integrate-and-fire model with diffusion noise, the steady state can be treated analytically (Tuckwell, 1989) but the distribution of firing times is not known. Our goal in this section is to identify a second noise model for which the interval distribution *can* be calculated, and which matches the diffusion noise model to a high degree of accuracy. Thus we consider two different ways to add noise to our model: first, the standard diffusion (noisy integration) process; next, an escape-rate process, represented in Fig. 3.

2.2.1. *Noisy integration (diffusion model)*

In this first noise model which we present for reference, noise is added to the integration process of an integrate-and-fire model (Stein, 1967; Tuckwell, 1989) according to the stochastic differential equation

$$\tau_m \frac{du}{dt} = -u(t) + R\,[I(t) + \xi(t)] \tag{6}$$

where $\xi(t)$ represents Gaussian white noise with zero mean and autocorrelation $\langle \xi(t)\xi(t')\rangle = \sigma_I^2 \delta(t-t')$ (and we have taken $R = 1$). If there were no threshold, the possible trajectories would have a Gaussian distribution about the noise-free reference trajectory, with variance $\sigma_u^2(t) = \left(R\sigma_I^2/(2\tau_m)\right)[1 - \exp(-2t/\tau_m)]$ (Tuckwell, 1989). With a threshold, however, the distribution of trajectories is non-Gaussian (due to the absorbing boundary at $u = \vartheta$). The interval distribution $P(t|\hat{t})$ given by the distribution of first passage times is known to be hard to calculate.

For constant input current $I(t) = I_0$, however, it is possible to calculate the mean interval, and hence to determine the effect of varying the mean potential $h_0 = RI_0$ on the mean rate. For integrate-and-fire neurons with diffusion noise, the mean interval $\langle T\rangle$ in the stationary state is given by (Johannesma, 1968; Tuckwell, 1989; Brunel and Hakim, 1999):

$$\begin{aligned}\langle T \rangle &:= \int s\, P(s|0)\, ds \\ &= \tau_m \int_0^\infty dv \frac{e^{-v^2}}{v} \left[e^{2vu_0} - e^{2vr} \right] \end{aligned} \tag{7}$$

where $u_0 = (\vartheta - h_0)/\sigma_0$ and $r = (\eta_{\text{reset}} - h_0)/\sigma_0$ with $\sigma_0 = R\sigma_I/\sqrt{\tau_m}$. The rate is simply $A_0 = 1/\langle T \rangle$.

Although we do not have an analytical result for the response to nonstationary inputs, [1] we can observe it in simulations by randomly applying a pulse to a neuron and accumulating the firing times into a PSTH. Each time the pulse is applied, there is an increased chance of a spike resulting in a peak in the PSTH after $t = 0$. Fig. 1, rows *d* and *e* show PSTHs derived from simulations of integrate-and-fire neurons with diffusion noise. We see that the shape of the PSTH response to a current pulse depends on the noise level. Before the pulse the neuron spikes at a constant mean firing rate determined by the mean input I_0 and the noise level. In the figure, the PSTH in row *d*, left column were obtained at a low noise level with a mean input that is above threshold. The input pulse increases the probability of spiking, resulting in a peak in the PSTH just after $t = 0$. A trough is visible immediately following the peak. The neuron fires tonically with a period of about 30 Hz; and a secondary peak occurs at $t = 33$ ms. Increasing the level of noise increased the baseline firing rate and decreased both the PSTH peak amplitude and the depth of the trough (row *d*, right column). For sufficiently high noise, the trough disappears. When the mean input is below threshold, a similar effect is observed (row *e*, left-hand column, low noise; upper trace in the right-hand column, high noise for the same I_0 as at left). Note that the changes in the peak and trough are not due to the change in baseline firing rate. To show this, we have readjusted the bias current I_0 in the high-noise regime to produce the same mean rate A_0 as in the low-noise regime (row *e*, right, lower trace). As can be seen by comparing the two traces, the shape and size of the peak hardly change (the secondary peak shifts as expected because of the change in the mean period).

2.2.2. *Noisy threshold (escape-rate model)*

We have seen that the noisy integration model displays the behavior we are trying to investigate, but is difficult to analyze in the general case.

[1] In standard integrate-and-fire neurons, the response to low-amplitude inputs could, in principle, be calculated using the methods as in (Brunel and Hakim, 1999).

We now introduce escape-rate noise models, which *can* be analyzed. After briefly describing a very simple model, the linear escape-rate noise model, we will present a noise model that behaves very much like the diffusion noise model.

Rather than adding noise explicitly to the membrane potential, we could simply view the spike-generation process itself as being stochastic. The escape-rate formulation provides a convenient way of doing this. Intuitively speaking, the probability of a spike at time t depends on the distance between the membrane potential and the threshold. More precisely, we introduce an escape rate f, which may be a function of the membrane potential u and of its derivative. Thus we can write $\rho_h(t|\hat{t})$, the hazard function given the net input potential $h(t|\hat{t})$ and the time of the last spike $\hat{t}$, in terms of f (Plesser and Gerstner, 2000):

$$\rho_h(t|\hat{t}) = f\left[u(t); \dot{u}(t)\right] \tag{8}$$

where $u(t) = \eta(t-\hat{t}) + h(t|\hat{t})$. This noise model may be viewed as corresponding to a stochastic threshold. Two specific escape rate functions f are presented in the following subsections. Before examining them we pause to make some general observations.

First we note that we may calculate the potential $u(t) = \eta(t-\hat{t}) + h(t|\hat{t})$ if the last firing time $\hat{t}$ and the input current $I(t)$ are known (Eq. 1). The advantage of this way of describing noise is that if we know the escape function f, we can calculate the hazard function ρ and hence the interval distribution (i.e. the probability density of firing at time t given that the last spike was at $\hat{t}$, in the presence of the input $h(t)$):

$$P_h(t|\hat{t}) = \rho_h(t|\hat{t}) \exp\left(-\int_{\hat{t}}^{t} \rho_h(t'|\hat{t}) dt'\right). \tag{9}$$

This probability density depends implicitly on $\hat{t}$ through Eqs. 2 and 8. The dependence on $\hat{t}$ enables us to take refractoriness into account. This model belongs to the class of renewal models; we can readily calculate the survivor function (Perkel et al., 1967; Cox, 1962) (i.e. the probability that a neuron does *not* fire between $\hat{t}$ and t) in the presence of the input h, $S_h(t|\hat{t}) = \exp(-\int_{\hat{t}}^{t} \rho(t'|\hat{t})\, dt')$. For later use, we now define $S_0(t-\hat{t})$, the survivor function for a constant input $h_0 = RI_0$. Then $S_0(t-\hat{t})$ is completely determined by the escape function f, the mean input potential h_0, and the refractory function $\eta(t-\hat{t})$. Examples of the interval distribution $P_h(t|\hat{t})$ and survivor function $S_h(t-\hat{t})$ are shown in Fig. 4 for the "Gaussian ISI" escape-rate model described later in this paper.

2.2.3. *Linear escape-rate noise model*

In the linear escape-rate model, the function f is piecewise linear. We express f in terms of the threshold ϑ and a rate ρ_1 of increase in firing rate above threshold :

$$f(u) = \begin{cases} \rho_{\min} & \text{for} \quad u(t) < \vartheta \\ \rho_{\min} + \rho_1(u - \vartheta) & \text{for} \quad u(t) \geq \vartheta \end{cases} \tag{10}$$

In the case of constant input $RI_0 \geq \vartheta$, the hazard function is

$$\rho_h(t|\hat{t}) = \begin{cases} \rho_{\min} & \text{for} \quad t - \hat{t} < t_{\text{refr}} \\ \rho_{\min} + \rho_1 \left[\eta(t - \hat{t}) + h_0(t - \hat{t}) - \vartheta\right] & \text{for} \quad t - \hat{t} \geq t_{\text{refr}} \end{cases} \tag{11}$$

where t_{refr} is given by the condition $\eta(t_{\text{refr}}) + h_0(t - \hat{t}) = \vartheta$. For $t \to \infty$ we find $\rho_h(t|\hat{t}) \to \rho_0 := \rho_{\min} + \rho_1 (RI_0 - \vartheta)$.

Fig. 5 shows the relations between the escape rate f, the potential u, and the hazard function ρ. Variants of the linear escape-rate model correspond to a single-memory Markov point process and are commonly used to describe the spike generation process, e.g. in auditory nerve fibers (Siebert and Gray, 1963; Miller and Mark, 1992). Above threshold, the linear escape rate model can give a good approximation of diffusion noise. The escape rate introduced in the next section is asymptotically linear for $u \gg \vartheta$.

2.2.4. *"Gaussian-ISI" escape-rate noise model*

This noise model gives a good approximation to the diffusion noise model. It is similar to the Arrhenius&Current noise model (Plesser and Gerstner, 2000) but is not restricted to the subthreshold regime.

To motivate this escape rate, we first examine the case in which a neuron is subjected to constant suprathreshold stimulation and its reference trajectory approaches threshold with nearly constant slope. This is, in fact, the typical situation in which experimental measurements of the effect of noise on the PSTH are carried out (Fetz and Gustafsson, 1983; Poliakov et al., 1996). The ISI distribution $P(t|\hat{t})$ will be very nearly Gaussian. Accordingly, we seek an escape rate function that yields a Gaussian distribution of interspike intervals,

$$\begin{aligned} P(t|\hat{t}) &= \frac{1}{\sigma_t\sqrt{2\pi}} \exp\left[-\frac{\left(t - \hat{t} - t_0\right)^2}{2\sigma_t^2}\right] & (12) \\ &\doteq G(t - \hat{t} - t_0, \sigma_t) & (13) \end{aligned}$$

where t_0 is the mean interval and σ_t is the width parameter of the temporal distribution. Making use of the relation $\frac{d}{dx}\left(\text{Erfc}\left(\frac{x}{\sqrt{2}\sigma_t}\right)\right) =$

$-2G(x, \sigma_t)$ where $\mathrm{Erfc}(x) = 1 - \mathrm{Erf}(x)$ is the complementary error function, we find the survivor function

$$S(t - \hat{t}) = \frac{1}{2}\mathrm{Erfc}\left(\frac{t - \hat{t} - t_0}{\sqrt{2}\sigma_t}\right). \tag{14}$$

From renewal theory, the hazard function must satisfy $S(t - \hat{t}) = \exp[-\int_{\hat{t}}^{t} \rho(t')dt']$ from which we find

$$\rho(t - \hat{t} - t_0) = 2\frac{G(t - \hat{t} - t_0, \sigma_t)}{\mathrm{Erfc}(\frac{t-\hat{t}-t_0}{\sqrt{2}\sigma_t})}. \tag{15}$$

To obtain the escape rate in terms of $(u - \theta)$ instead of $t - \hat{t} - t_0$, we make the following linear approximation near threshold. Suppose that the membrane potential passes threshold at t_0, i.e. $u(t_0) = \vartheta$. Then $u(t - \hat{t}) = \vartheta - (du/dt)|_{t_0}(t - \hat{t} - t_0) \Rightarrow t - \hat{t} - t_0 = (u - \theta)/(du/dt)|_{t_0}$. Hence the desired escape rate is of the form

$$f(u - \theta) = 2 \left.\frac{du}{dt}\right|_{t_0} \frac{G(u - \theta, \sigma_u)}{\mathrm{Erfc}(\frac{u-\theta}{\sqrt{2}\sigma_u})} \tag{16}$$

(using $\sigma_u = \sigma_t(du/dt)|_{t_0}$). In the limit of $u \gg \vartheta$, f asymptotically approaches $(u - \theta)(du/dt)|_{t_0}/\sigma_u^2$.

Eq. 16 has been motivated above for the suprathreshold regime. In the subthreshold regime the escape rate is expected to be proportional to $G(u - \theta, \sigma_u)$, i.e. the free density at threshold (Plesser and Gerstner, 2000). If we divide G by Erfc, the escape rate continues to increase above threshold as it should.

Taking together both the above Gaussian escape rate and the term on the right-hand side of Eq. 16, we arrive at the escape rate

$$f(u - \theta) = w\left(\frac{1}{\tau} + 2u'H[u']\right)\frac{G(u - \theta, \sigma_u)}{\mathrm{Erfc}(\frac{u-\theta}{\sqrt{2}\sigma_u})} \tag{17}$$

which we will use throughout this paper, where $u' = (du/dt)$ evaluated at t and w is a parameter. The first term describes the escape rate for constant subthreshold or slowly varying inputs; the second term gives the escape rate for rapidly varying or suprathreshold inputs; and the constant w is an overall factor to be optimized. The $H[u']$ term precludes firing on downward strokes. Optimization was performed using the procedure described in (Plesser and Gerstner, 2000): the median value was chosen from the optimal weights determined for a large set of periodic and aperiodic stimuli; the optimal value is $w = 1.21$ (H.

E. Plesser, private communication). Fig. 4 shows the escape rate as a function of membrane potential.

3. Results

Using the noisy neuron model defined above we can predict the probability of a spike given (a) the input and (b) the initial conditions. How do we predict the PSTH? Recall that in experiments, the PSTH is measured for a single neuron as follows: a stimulus is presented many times and the histogram of spike times or PSTH is calculated and expressed as a firing rate. Each time the stimulus is presented, the initial condition of the neuron is not known. Thus, the PSTH is the probability of a spike given *random* initial conditions. In the following section we apply a theory of population activity that will allow us to move from known to random initial conditions, and so to predict the PSTH. We then apply this theoretical result to the integrate-and-fire neuron model. In Sec. 3.2.2 we compare theoretical predictions with simulations.

3.1. Theoretical results

3.1.1. *From a noisy population to the PSTH of a single noisy neuron*
Consider a homogeneous population of N unconnected, noisy neurons initialized with random initial conditions, all receiving the same input. Since the neurons are fully independent and their phases are unsynchronized (incoherent state), the activity of the population as a whole in response to a given stimulus is equivalent to the PSTH compiled from the response of a single noisy neuron to N repeated presentations of the same stimulus. Hence, we can apply theoretical results for the activity of homogeneous populations to the PSTH of an individual neuron. This section summarizes the theory.

The theory in (Gerstner, 1995; Gerstner, 2000) describes the proportion $A(t)$ of active neurons in a population of size N (i.e. the population-averaged activity) of a large, homogeneous, randomly initialized population of neurons. Formally, we define

$$A(t) = \lim_{\Delta t \to 0} \frac{1}{\Delta t} \frac{n_{\mathrm{act}}(t; t + \Delta t)}{N} \tag{18}$$

where $n_{\mathrm{act}}(t; t + \Delta t)$ is the number of neurons that emitted a spike between t and $t + \Delta t$; N is the total number of neurons in the population. The population dynamics are given in terms of (a) the net input potential generated by the input applied to the entire population and

(b) the previous activity of the population, in the following integral equation:

$$A(t) = \int_{-\infty}^{t} P_h(t|\hat{t}) A(\hat{t}) d\hat{t} \tag{19}$$

where $P_h(t|\hat{t})$ is the probability density describing the probability of firing for each neuron at time t, given that the neuron has fired at a previous time $\hat{t}$, driven by the net input potential $h(t|\hat{t})$. Experimentally, $P_h(t|\hat{t})$ is estimated using the ISI (inter-spike interval) histogram. In the escape noise model, $P_h(t|\hat{t})$ is given by Eq. 9.

Eq. 19 gives the exact response and is nonlinear. It may be evaluated numerically for specific choices of noise models and neuron models. An algorithm for calculating the full response for the integrate-and-fire neuron with an escape rate noise model is given in the Appendix. However, the relation between the response and the input is not explicitly clear. Fortunately, as we show next, expansion of Eq. 19 to first order in the signal ΔI yields a fair approximation of the response explicitly in terms of the postsynaptic potential.

Consider a single neuron to which a constant input I_0 is applied, producing a mean firing rate A_0. If we now add a small current pulse $\Delta I(t)$, the membrane potential will be perturbed by an amount $\Delta h(t|\hat{t}) = \int_0^\infty \varepsilon(t-\hat{t}, s)\Delta I(t-s)ds$. Since this perturbation can be identified with the postsynaptic potential we write $PSP(t|\hat{t})$ for $\Delta h(t|\hat{t})$. Notice that it explicitly depends on the last firing time $\hat{t}$.

We are going to determine the PSTH of the neuron by calculating $A(t) = A_0 + \Delta A(t)$. Thus A_0 is the baseline firing level of the PSTH and $\Delta A(t)$ describes the peak.

3.1.2. *Constant input*

The reference point A_0 of the linearization is the mean activity of a population receiving a constant input. [2] Let us denote the interval distribution in this case by $P_0(t|\hat{t})$. We can write the mean activity as the inverse of the mean interval, i.e.:

$$A_0 \;=\; \left\{ \int_0^\infty s\, P_0(\hat{t}+s|\hat{t}) ds \right\}^{-1} \tag{20}$$

Fig. 6 plots the mean firing rates for the integrate-and-fire neuron with the "Gaussian ISI" noise model, for high and low noise. They are compared with the rates for the noisy integration model (cf. Eq. 6).

[2] Even if the population is not initialized to have a constant activity A_0, provided the neuron model includes sufficient noise, the noise will eventually suppress oscillations and the activity of the population will become practically constant (for N sufficiently large).

3.1.3. *Impulse response*

Now we add a fluctuation to the previously constant input. The fluctuation could be a postsynaptic current pulse. In terms of the input current, we write $I(t) = I_0 + \Delta I(t)$. The input potential becomes $h(t|\hat{t}) = h_0(t|\hat{t}) + PSP(t|\hat{t})$, where $PSP(t|\hat{t}) = \Delta h(t|\hat{t})$. The population activity will respond by undergoing a transient $A(t) = A_0 + \Delta A(t)$ before decaying back to the original level A_0. The shape of the transient $\Delta A(t)$ depends on the size (and duration) of the input pulse, the particular noise model, and the population activity itself (Gerstner, 2000):

$$\begin{aligned}\Delta PSTH(t) &= (\text{influence of past perturbations}) \\ &\quad + \frac{d}{dt}(\text{a filtered version of the potential})\end{aligned}$$

or

$$\begin{aligned}\Delta A(t) &= \int_{-\infty}^{t} d\hat{t}\, P_{h_0}(t|\hat{t})\, \Delta A(\hat{t}) \\ &\quad + A_0 \frac{d}{dt} \left\{ \int_{-\infty}^{t} dt_1 \int_{-\infty}^{t} d\hat{t}\; PSP(t_1|\hat{t}) \mathcal{F}(t-\hat{t}, t_1-\hat{t}) \right\} \qquad (21)\end{aligned}$$

where $\mathcal{F}(t-\hat{t}, t_1-\hat{t}) = \left.\frac{\partial S_h(t|\hat{t})}{\partial PSP(t_1|\hat{t})}\right|_{PSP=0}$.

3.2. Application to integrate-and-fire neurons

The above is a very general result and needs to be evaluated for a specific model. In this section we apply it to the integrate-and-fire neuron model using the "Gaussian ISI" escape rate noise model and compare theory with simulations.

3.2.1. *Interpretation of theoretical results*

For the integrate-and-fire neuron the impulse response may be written in the following form (Gerstner, 2000):

$$\Delta A(t) = \int_{-\infty}^{t} d\hat{t}\, P_{h_0}(t|\hat{t})\, \Delta A(\hat{t}) + A_0 \frac{d}{dt} \left[\int_0^{\infty} dx\, L(x)\, PSP(t-x) \right] \qquad (22)$$

where $PSP(t)$ is the postsynaptic potential for a neuron whose last firing time $\hat{t} = -\infty$ (i.e. $PSP(t) = \int_0^{\infty} \epsilon(\infty, s) \Delta I(t-s) ds$ $= \int_0^{\infty} \exp(-s/\tau_m)\; \Delta I(t-s) ds$). Note that the $\hat{t}$ has disappeared from the second term, which now is a simple convolution of the PSP with the filter L.

For the "Gaussian ISI" noise model (cf. Eq. 17) with the neuron described in Section 2.1, we have $L(x) = L_1(x) + L_2(x) \cdot \frac{d}{dt}$, where

$$\begin{aligned} L_1(x) \;&=\; \int_x^\infty \frac{\partial f}{\partial u}\left[u_0(\hat{x}-x); u_0'(\hat{x}-x)\right]\, S_0(\hat{x})\, d\hat{x} \\ &\quad -S_0(x)\int_0^x e^{-\hat{x}/\tau_\mathrm{m}} \frac{\partial f}{\partial u}\left[u_0(\hat{x}-x); u_0'(\hat{x}-x)\right]\, d\hat{x}, \\ L_2(x) \;&=\; \int_x^\infty \frac{\partial f}{\partial u'}\left[u_0(\hat{x}-x); u_0'(\hat{x}-x)\right]\, S_0(\hat{x})\, d\hat{x} \\ &\quad -S_0(x)\int_0^x e^{-\hat{x}/\tau_\mathrm{m}} \frac{\partial f}{\partial u'}\left[u_0(\hat{x}-x); u_0'(\hat{x}-x)\right]\, d\hat{x}. \end{aligned} \tag{23}$$

Here u_0 refers to the unperturbed membrane potential, $u_0(t-\hat{t}) = \eta(t-\hat{t}) + h_0$, and S_0 is the pre-pulse survivor function defined in Section 2.2.2. These integrals can be evaluated numerically using the derivatives $\partial f/\partial u$ and $\partial f/\partial u'$ obtained from the definition of the escape rate, and S_0 defined in Section 2.2.2, also calculated from the escape rate. The response can conveniently be calculated numerically from Eq. 22 using fast Fourier transforms. For the calculation of $\partial f/\partial u'$ we neglect the step function $H(u')$ in order to have a truly linear theory (in contrast to a piecewise linear theory).

Eq. 22 is the central result of our theory. It relates the form of the predicted PSTH, $PSTH(t)$, to the form of the PSP. It may be helpful to refer back to Fig. 1 in order to understand this relation.

In Eq. 22, the first term on the right-hand side describes the influence of past perturbations. When the noise level is low and stimulation strong, this term can generate a small secondary peak at a delay corresponding to the mean period $1/A_0$.

The contribution of the second term of Eq. 22 to the response is determined by the filter L. The sharpness of L depends on the noise level via the stationary survivor function S_0. To simplify the discussion let us neglect the term L_2. If there is no noise, L is a δ-function and the second term in (22) becomes proportional to $\frac{d}{dt}PSP(t)$ (left column, center trace in Fig. 1); a trough appears following the primary peak because neurons that fired during the peak are refractory. Note that if the slope of the membrane trajectory u' is constant between spikes, in the noiseless case this term reduces to $A_0\frac{d}{dt}PSP(t)/u'$. If there is a lot of noise, L becomes broad, effectively canceling the derivative. The term becomes more like $PSP(t)$ (right column, center trace in Fig. 1) and the trough disappears. For intermediate noise levels the behavior is somewhere between these extremes (cf. the right-hand simulation of Fig. 1).

3.2.2. *Comparison with simulations*
Numerically calculated filters L are shown for various levels of noise in Fig. 7. These were used to predict the responses to α-function shaped pulses of external current. Fig. 8 compares the predictions made using the linear filter calculated for the integrate-and-fire neuron and the "Gaussian ISI" noise model with simulations of the same model together with predictions obtained from the full nonlinear model (Eq. 19) using the algorithm outlined in the Appendix. It can be seen that although the full model produces asymmetric responses to symmetric positive and negative input pulses, the linear filter of course produces symmetric responses. Fig. 9 compares the linear predictions made using the filter calculated for the "Gaussian ISI" noise model with simulations made using the noisy integration model (Eq. 6). The linear model reproduces the essential features we wanted to explain. In particular, for both models simulated, the activity in high noise has a peak resembling the PSP, whereas activity in the low-noise cases clearly shows the characteristic trough following the peak from the influence of the PSP derivative.

We explored the domain of validity of the linear model defined by Eq. 22 by simulating input pulses of various sizes and measuring the height of the resulting peaks for the noisy integration model. We found good agreement between theory and simulations for positive pulses, summarized in Fig. 10. Nonlinear effects can be observed: the response to excitatory and inhibitory PSPs is not symmetric (also in Fig. 9). These nonlinearities are accurately described by the full nonlinear theory. A similar asymmetry is seen in motoneuron experiments (Fetz and Gustafsson, 1983; Poliakov et al., 1997).

We also explored the effect of varying the mean input level I_0 on the peak amplitude $|\Delta A|$ at different noise levels. The relationships between I_0 and both the background rate A_0 and $|\Delta A|$ are summarized in Fig. 11. Over the input range shown, the amplitude of the peak is fairly sensitive to the noise level σ_u, but relatively insensitive to the drive level I_0. The low-noise response has a maximum at about $RI_0 = \vartheta - \sigma_u$, similar to results reported previously for oscillatory input (Kempter et al., 1998; Plesser and Tanaka, 1997) and suggesting the possibility of a stochastic resonance effect (Gammaitoni et al., 1998).

To summarize, the analytical results calculated for the "Gaussian ISI" escape rate model give a good fit to simulated noisy integration model responses to pulse inputs, across a wide range of noise conditions. The asymmetric response of the noisy integration model is captured in the full nonlinear model (Eq. 19) but not in the linear filter approximation.

4. Discussion

A number of studies have documented the effect of noise on the probability of firing following a stimulus (which could be a presynaptic spike, a current, or a PSP) (Midroni and Ashby, 1989; Kenyon et al., 1992). However, no theory has been proposed to date explicitly incorporating both a noise model and arbitrary functions for the PSP and afterhyperpotential.

4.1. General theory

We have developed a theory based on a rather general neuron model that can accomodate arbitrary forms for the input, the membrane response and the spike afterpotential. However, the theory incorporates a voltage threshold which is not accurate in case of very slowly varying input (Koch, 1999). Variations in spike threshold have been observed experimentally in motoneurons (Calvin, 1974; Schwindt and Crill, 1982; Powers and Binder, 1996). Threshold variations that depend on the last firing time $\hat{t}$ can be accomodated in the spike response model by incorporating them into the η-kernel; input-dependent threshold changes, however, cannot. In particular, adaptation is not taken into account in the spike-response model.

The linear filter theory allows a clear interpretation of the relation between the shape of the PSTH and the PSP. Since it is based on a linearization of the response to a small pulse, it cannot account for observed departures from linearity such as asymmetric responses to positive and negative pulses (Fig. 10). Our full nonlinear theory, however, captures these asymmetries.

4.2. Limitations of the integrate-and-fire model

To illustrate our results, we have reduced the complexity of the model to a minimum in order to show that the phenomenon of noise dependence of the PSTH response to an input pulse does not depend on detailed cell properties with particular parameter values. The integrate-and-fire model has only one time constant; choosing its value to be the experimentally measured passive time constant produces highly unrealistic membrane potential trajectories for tonic firing (when the mean input is suprathreshold). In the companion article (Herrmann and Gerstner, 2000) we study a simple extension of the integrate-and-fire neuron with three time constants, yielding more realistic behavior.

In this article we have chosen $\tau_m = 4$ ms; we interpret this as an "effective" membrane time constant during spontaneous activity (Bernander et al., 1991).

A further limitation of the model is that the description of the synaptic input by current pulses necglects the influence of the synaptic reversal potential. In our integrate-and-fire model, the current pulse has the same effect whether the membrane potential is at rest or close to threshold. In the slow recovery model presented in the companion paper, the postsynaptic potential $\epsilon(t-\hat{t}, s)$ depends on the time elapsed since the last spike, $t - \hat{t}$, and mimics conductance changes along the membrane potential trajectory.

4.3. Predictions of the model

With the analysis presented here we have attempted to explain some experimental results obtained for tonic firing in motoneurons. This is because the only experiments we are aware of in which PSTHs are recorded under controlled noise conditions have been performed on motoneurons. We make specific predictions about motoneurons in the companion paper (Herrmann and Gerstner, 2000). However, because our neuron description is so general, we predict that the effect of noise on the PSTH response to input spikes should be observable in most types of neurons. Specifically observable effects are:

1. The shape of the PSTH response to an input spike can be predicted using the method presented in this paper using experimentally measured kernels of the spike-response model, subject to the limitations discussed above. The kernels can be determined using the methods in (Kistler et al., 1997).

2. Noise affects the PSTH as follows: In low noise, the shape of the PSTH should exhibit a trough following the main peak due to refractoriness; if the mean input is kept constant, increasing the noise level both increases the mean firing rate and decreases the amplitude of the peak and the trough. If the mean input is adjusted so that the mean firing rate stays the same, the amplitude of the peak and trough also decrease. Furthermore, this effect should be observable both for tonic and irregular firing modes (above and below threshold).

3. At low noise levels, the PSTH peak amplitude reaches a maximum when the mean input is below threshold and the neuron is firing irregularly; if the mean input decreases further, the PSTH peak falls off rapidly. Increasing the amount of noise can extend the range of response below threshold.

5. Conclusions

In simulations we have shown that in integrate-and-fire neurons with diffusion noise (noisy integration), the amount of background noise affects the shape of the PSTH response to an input spike in the same way as in analogous experiments with motoneurons. To understand the process, we developed an escape-rate noise model that approximates noisy integration. This model allows the form of the response to be predicted based on the shape of the postsynaptic current pulse. The results show good agreement with the noisy integration model and demonstrate that it is possible to take into account both the amount of noise and the shape of the membrane trajectory. For low noise levels, the response clearly has a strong component from the derivative of the postsynaptic potential: the primary peak is followed by a distinct trough and secondary peaks, even when the neuron is not firing tonically. For higher noise levels, the trough and secondary peaks disappear and the PSTH resembles the PSP rather than its derivative.

Thus by using the spike response formalism to describe neuronal dynamics, an escape rate noise model, and population theory to map the single-trial response to the PSTH, we were able to show how the noise level controls the shape of the PSTH. We obtained results that are analogous to the experimental results of Poliakov et al. (1996) in motoneurons in the suprathreshold regime and predict that they should extend to the subthreshold regime, and to other neurons as well.

6. Appendix

We present here an algorithm for calculating the predicted PSTH of an integrate-and-fire neuron with escape rate noise responding to an input pulse superimposed on a constant background level. This algorithm, based on the procedure outlined in Appendix A of (Gerstner, 2000), is derived from the integral population equation repeated here for convenience:

$$A(t) = \int_{-\infty}^{t} P_h(t|\hat{t}) A(\hat{t}) d\hat{t} \tag{24}$$

To evaluate this integral we shall 1) determine the interval distribution $P_h(t|\hat{t})$ in terms of the input current $I(t)$ using the escape-rate noise model and spike response neuron model, and 2) transform the above infinite integral into a finite one, then discretize it.

For an escape-rate noise model, the interval distribution may be written in terms of the escape rate and the survivor function, $P_h(t|\hat{t}) = f[u(t|\hat{t})]S_h(t|\hat{t})$.

We have defined the integrate-and-fire neuron in the form $u(t - \hat{t}) = \eta(t - \hat{t}) + h(t|\hat{t})$. The input potential is related to the input current through $h(t|\hat{t}) = h_{\text{free}}(t) + h_{\text{free}}(\hat{t}) \exp[-(t-\hat{t})]$ where $h_{\text{free}}(t) = \int_0^\infty \epsilon(s) I(t-s) ds$ does not depend on the last spike time (Gerstner, 2000).

Noting that the refractory function η vanishes if we wait long enough after a spike, we define a time interval Δ_{free} such that $\eta(t-\hat{t}) \approx 0$ and $h(t|\hat{t}) \approx h_{\text{free}}(t)$ for $t - \hat{t} > \Delta_{\text{free}}$. In this case, since the membrane potential no longer depends on the time of the last spike, the hazard function does not either and we can write $P_h(t|\hat{t}) \to f[h_{\text{free}}(t)]S_h(t|\hat{t})$ for $t - \hat{t} > \Delta_{\text{free}}$. We therefore decompose the population equation into refractory and post-refractory ("free") epochs:

$$\begin{aligned} A(t) &= \int_{-\infty}^{t-\Delta_{\text{free}}} P_h(t|\hat{t})A(\hat{t})d\hat{t} + \int_{t-\Delta_{\text{free}}}^{t} P_h(t|\hat{t})A(\hat{t})d\hat{t} \\ &= f[h_{\text{free}}(t)] \int_{-\infty}^{t-\Delta_{\text{free}}} S_h(t|\hat{t})A(\hat{t})d\hat{t} \\ &\quad + \int_{t-\Delta_{\text{free}}}^{t} f[u(t|\hat{t})]S_h(t|\hat{t})A(\hat{t})d\hat{t} \end{aligned} \tag{25}$$

One last transformation must be made. Applying the normalization $\int_\infty^t S_h(t|\hat{t})A(\hat{t})d\hat{t} = 1$ (Gerstner, 2000), we obtain the finite integral (see also Wilson and Cowan (1972))

$$\begin{aligned} A(t) &= f[h_{\text{free}}(t)] \left\{ 1 - \int_{t-\Delta_{\text{free}}}^{t} S_h(t|\hat{t})A(\hat{t})d\hat{t} \right\} \\ &\quad + \int_{t-\Delta_{\text{free}}}^{t} f[u(t|\hat{t})]S_h(t|\hat{t})A(\hat{t})d\hat{t}. \end{aligned} \tag{26}$$

We now discretize into time steps t_i of length dt; for each t_i we define the j-th "delay" $\Delta_j = j\ dt$ so that $t_i - \hat{t}_j = j\ dt = \Delta_j$. We identify the following quantities to evaluate at each t_i:

- $P_{\text{free}}(t_i) = \{1 - \exp(-f[h(t_i), h'(t_i)])\}\ dt$, the probability of firing in the time interval at t_i for neurons that are post-refractory

and the *vectors*

- $P(\Delta_j) = \{1 - \exp(-f[u(t_i|\hat{t}_j), u'(t_i|\hat{t}_j)])\}\ dt$, the probability of firing in the time interval at t_i for neurons that last fired at time $\hat{t}_j = t_i - \Delta_j$

- $n(\Delta_j) = S_h(t_i|t_i - \Delta_j)A(\hat{t}_j)dt$, the fraction of neurons that fired last at time $\hat{t}_j = t_i - \Delta_j$
- $m(\Delta_j) = P(\Delta_j)n(\Delta_j)dt$, the fraction of neurons having last fired at $\hat{t} = t_i - \Delta_j$ that fire at time t_i

where the delay Δ_j ranges from 0 to Δ_{free} in steps dt. Note that n must always satisfy $\sum_{\Delta_j} n(\Delta_j) = 1$, and $m(0) = 0$. The algorithm consists of iteratively evaluating the discretized version of Eq. 26,

$$A(t_i)\ dt \ = \ f[h_{\text{free}}(t_i)]\ dt \left(1 - \sum_{\Delta_j} n(\Delta_j)\right) + \sum_{\Delta_j} m(\Delta_j), \quad (27)$$

as follows:

1. Determine Δ_{free} such that $\eta(t - \hat{t}) \approx 0$ and $h(t|\hat{t}) \approx h_{\text{free}}(t)$ for $t - \hat{t} \geq \Delta_{\text{free}}$.
2. Initialize $t_i = t_0$. Initialize the vector $h_{\text{free}}(\Delta_j)$ for the delays $0 \leq t_j < \Delta_{\text{free}}$ using $h_{\text{free}}(t_i < t_0) = h_{\text{free}}(t_0)$.
3. Compute the vectors $\eta(\Delta_j) = -\eta_0 \exp(-\Delta_j/\tau_m)$ and $h(\Delta_j) = h_{\text{free}}(\Delta_j)[1 - \exp(-\Delta_j/\tau_m))]$ for neurons that last fired at $t_0 - \Delta_j$.
4. Initialize the activity vector $n(\Delta_j)$ using $u_0(\Delta_j) = h(\Delta_j) + \eta(\Delta_j)$, $u'_0(\Delta_j) = [\eta(\Delta_j) - \eta(\Delta_{j-1})]/dt$, and the stationary survivor function S_0 as follows:

   a) Compute the vector $S_0(\Delta_j)$:
   $S_0(0) = 1$; for $0 < (\Delta_j) < \Delta_{\text{free}}$,
   $S_0(\Delta_j) = \{1 - dt\ f[u_0(\Delta_j), u'_0(\Delta_j)]\}\ S_0(\Delta_{j-1})$.

   b) $A_0 = [\sum_{\Delta_j} S_0(\Delta_j)\ dt]^{-1}$.

   c) $n(\Delta_j) = A_0\ S_0(\Delta_j)\ dt$.

5. For each time step t_i:

   a) For each Δ_j, update the vectors:

   i) $h_{\text{free}}(\Delta_j)$ from the input $I(t_i)$ as defined above, using:
   $h_{\text{free}}(0) = h_{\text{free}}(0)(1 - dt/\tau_m) + (dt/\tau_m)I(t_i)$;
   for $0 < \Delta_j < \Delta_{\text{free}}$, $h_{\text{free}}(\Delta_j) = h_{\text{free}}(\Delta_{j-1})$

   ii) $h(\Delta_j) = h_{\text{free}}(t_i) - \exp(-\Delta_j/\tau_m)h_{\text{free}}(t_i - \Delta_j)$

   iii) $P(\Delta_j)$ as defined above, using $u(\Delta_j) = h(\Delta_j) + \eta(\Delta_j)$ and $du = h(t_i) - h(t_{i-1}) + \eta(t_i) - \eta(t_{i-1})$

   iv) $m(\Delta_j)$ as defined above.

b) Update $P_{\mathrm{free}}(t_i)$ as defined above.

c) Compute $A(t_i) = P_{\mathrm{free}}(t_i)[1 - \sum_{\Delta_j} n(\Delta_j)] + \sum_{\Delta_j} m(\Delta_j)$.

d) Update the vector $n(\Delta_j)$:
$n(0) = A(t_i)$; for $0 < \Delta_j < \Delta_{\mathrm{free}}$, $n(\Delta_j) = n(\Delta_{j-1}) - m(\Delta_{j-1})$.

Our implementation of the above algorithm on a Pentium-II class computer simulates 100 ms of population activity ms in under 3 seconds of computer time using $dt = 0.05$.

References

Abeles M. *Corticonics*, Cambridge University Press, Cambridge, 1991.

Bernander Ö, Douglas RJ, Martin KA, Koch C. Synaptic background activity influences spatiotemporal integration in single pyramidal cells. *Proc. Natl. Acad. Sci. USA*, 88:11569–11573, 1991.

Brunel N, Hakim V. Fast global oscillations in networks of integrate-and-fire neurons with low firing rates. *Neural Computation*, 11:1621–1671, 1999.

Calvin WH. Three modes of repetitive firing and the role of threshold time course between spikes. *Brain Res.*, 59:341–346, 1974.

Cox DR. *Renewal theory*, Methuen, London, 1962.

Fetz EE, Gustafsson B. Relation between shapes of post-synaptic potentials and changes in firing probability of cat motoneurones. *J Physiol*, 341:387–410, 1983.

Gammaitoni L, Hänggi P, Jung P, Marchesoni F. Stochastic resonance. *Rev. Mod. Phys.*, 70:223–287, 1998.

Gerstner W. Time structure of the activity in neural network models. *Phys. Rev. E*, 51(1):738–758, 1995.

Gerstner W. A framework for spiking neuron models - the spike response method (Preprint), 1999. To appear in: Gielen S. et al., eds., *The Handbook of Biological Physics*. Elsevier. Available at http://diwww.epfl.ch/lami/team/gerstner/.

Gerstner W. Population dynamics of spiking neurons: fast transients, asynchronous states and locking. *Neural Computation*, 12:1–46, 2000.

Herrmann AK, Gerstner W. Noise and the PSTH response to current transients: II. Application to motoneuron data. Submitted to *J. Comp. Neurosci.*.

Johannesma PIM. Diffusion models of the stochastic activity of neurons. In E R Caianello (Ed.), *Neural Networks*, pp. 116–144. Springer, Berlin, 1968.

Kempter R, Gerstner W, van Hemmen JL, Wagner H. Extracting oscillations: Neuronal coincidence detection with noisy periodic spike input. *Neural Computation*, 10:1987–2017, 1998.

Kenyon GT, Puff RD, Fetz EE. A general diffusion model for analyzing the efficacy of synaptic input to threshold neurons. *Biol. Cybern.*, 67 (2):133–41, 1992.

Kirkwood PA, Sears TA. The synaptic connexions to intercostal motoneurones as revealed by the average common excitation potential. *J Physiol*, 275:103–134, 1978.

Kistler WM, Gerstner W, van Hemmen JL. Reduction of Hodgkin-Huxley equations to a single-variable threshold model. *Neural Computation*, 9:1015–1045, 1997.

Koch C. *Biophysics of computation*, Oxford University Press, New York, 1999.

Knox CK. Cross-correlation functions for a neuronal model. *Biophysical Journal*, 14:567–582, 1974.

Midroni G, Ashby P. How synaptic noise may affect cross-correlations. *J. Neurosci. Meth.*, 27:1–12, 1989.

Miller MI, Mark KE. A statistical study of cochlear nerve discharge patterns in response to complex speech stimuli. *J. Acoust. Soc. Am*, 92:202–209, 1992.

Moore GP, Segundo JP, Perkel DH, Levitan H. Statistical signs of synaptic interaction in neurons. *Biophysical Journal*, 10:876–900, 1970.

Perkel DH, Gerstein GL, Moore GP. Neuronal spike trains and stochastic point processes I. The single spike train *Biophysical Journal*, 7:391–418, 1967.

Plesser HE, Gerstner W. Noise in integrate-and-fire neurons: from stochastic input to escape rates. *Neural Computation*, 12: 367–384, 2000.

Plesser HE, Tanaka S. Stochastic resonance in a model neuron with reset. *Phys. Lett. A*,225: 228–234, 1997.

Poliakov AV, Powers RK, Binder MD. Functional identification of the input–output transforms of motoneurones in the rat and cat. *J. Physiol.*, 504 (Pt 2):401–424, 1997.

Poliakov AV, Powers RK, Sawczuk A, Binder MD. Effects of background noise on the response of rat and cat motoneurones to excitatory current transients. *J. Physiol.*, 495 (Pt 1):143–157, 1996.

Powers RK, Binder MD. Experimental evaluation of input-output models of motoneuron discharge. *J. Neurophysiol.*, 75:367–379, 1996.

Schwindt PC, Crill WE. Factors influencing motoneuron rhythmic firing: results from a voltage-clamp study. *J. Neurophysiol.*, 48:875–890, 1982.

Siebert WM, Gray PR. Random process model for the firing pattern of single auditory neurons. *Q. Prog. Rep., Res. Lab. of Elec. MIT*, 71:241, 1963.

Stein RB. Some models of neuronal variability. *Biophys. J.*, 7:37–68, 1967.

Tuckwell HC. *Stochastic Processes in the Neurosciences*. SIAM, Philadelphia, 1989.

Wilson HR, Cowan JD. Excitatory and inhibitory interactions in localized populations of model neurons. *Biophys. J.*, 12:1–24, 1972.

7. Figure Legends

7.1. Figure 1

Effect of noise on the PSTH. A neuron responds to a current transient, $I(t) = I_0 + \Delta I(t)$ (a, arbitrary units) with an increased spiking probability, measured via the PSTH. **Left column**, "low noise"; **Right column**, "high noise". Row b, the noisy current input including diffusive noise simulating uncorrelated background input. The time course of the noisy input current is the same in both columns; only the noise amplitude σ_u has been changed. Row c, time course of the PSP derivative (arbitrary scale). Rows d and e, PSTHs obtained from a simulation of a standard integrate-and-fire neuron with diffusive noise, Eq. 6 using the baseline input current levels I_0 indicated in the plots. In row d, RI_0 is above threshold and the neuron fires tonically; in row e, $RI_0 < \vartheta$ and the neuron fires irregularly. Very high peak amplitudes can be observed in low noise when the mean input is about 1 σ_u below threshold. In row e, left, the peak has been clipped; its amplitude is 1133 Hz.

Simulation parameters: threshold $\vartheta = 0$, $R = 1$, $\tau = 4$ ms, $\eta_0 = 1$. "Low noise" $\sigma_u = 2.2\ 10^{-5}$, "high noise" $\sigma_u = 7.07\ 10^{-4}$. Input pulse amplitude $\Delta I(t) = 0.001(t/\tau_r)\exp(1 - t/\tau_r)$ where $\tau_r = 0.5$ ms. Time step 0.1 ms averaged to 0.2 ms; 50,000 stimulus presentations.

7.2. Figure 2

The spike-response model (solid curve) approximates a spike and its afterpotential (dashed) using a template-like refractory kernel, $\eta(t - \hat{t})$ (inset). The refractory kernel is applied whenever the membrane potential $u(t)$ reaches the threshold ϑ, causing a spike. In the example shown here (which corresponds to the integrate-and-fire model), the spike at time $\hat{t}$ is a formal event and its form has been reduced to a delta function. The kernel η causes the membrane potential u to be reset and then to decay exponentially. Other kernels, not presented here, can provide better approximations to real action potentials and afterhyperpolarizations (Kistler et al., 1997).

7.3. Figure 3

Two ways of adding noise to an integrate-and-fire model. **Left:** in noisy integration, diffusion noise is added to the membrane potential during the integration process. The actual trajectory (solid line) drifts away from the noise-free reference trajectory (dashed). When the potential reaches threshold, a spike is generated and the potential is reset. Spike occurences are symbolized by the solid upwards arrows. **Right:**

in an escape-rate formulation, noise is represented through a hazard function: the neuron can spike even when the membrane potential is below threshold. The probability of firing $\rho(t)$ (large arrow) depends on the instantaneous distance to threshold. When a spike occurs, the membrane potential is reset and follows the reference trajectory until the next spike. Both diagrams are for constant input current $I(t) = I_0$.

7.4. Figure 4

Top, escape rate as a function of the normalized potential distance to threshold $(u - \vartheta)/(\sqrt{2}\sigma_u)$, calculated using Eq. 17. Dotted, $u' = 1$; dashed, $u' = 0.5$; solid, $u' = 0$.

Bottom left, interval distributions $P_h(t|\hat{t})$; bottom right, survivor functions $S_h(t-\hat{t})$ for the integrate-and-fire neuron calculated using the "Gaussian ISI" escape rate, Eq. 17. Dashed lines, high noise ($\sigma_u = 1$); solid lines, low noise ($\sigma_u = 0.005$). The threshold is 0 in both cases; the input potential level h_0 was adjusted to give the same mean firing rate for both noise levels $A_0 \approx 30$ Hz.

7.5. Figure 5

Escape function $f(u)$, membrane potential after a spike $u(t)$, and hazard function $\rho(t)$ in the presence of a constant input $h_0 = RI_0$. Top row, the input is below threshold, $h_0 < \vartheta$. Bottom row, $h_0 > \vartheta$. (a) Thick curves: In the linear escape function $f(u)$, the firing rate is $\rho_{\min}$ below threshold; for $u > \vartheta$ it increases with u, with slope ρ_1. Thin curves: nonlinear, diffusion-like escape function. A constant input potential h_0 results in a 'background firing level' $f(h_0)$. For the linear escape function, when $h_0 < \vartheta$ (top), $f(h_0) = \rho_{\min}$. (b) An example of a membrane potential trajectory $u(t)$. A spike occurs at time $\hat{t}$, generating a refractory potential. (c) The resulting hazard function $\rho_h(t|\hat{t})$. Thick curves: For the linear escape function, when $h_0 < \vartheta$ (top), the hazard function does not change after a spike; when $h_0 > \vartheta$ (bottom), the hazard function is clamped at $\rho_{\min}$ following the spike until the membrane potential u again crosses threshold. Thin curves: The hazard function for the nonlinear, diffusion-like escape function is modulated by the refractory function, but only weakly for $RI_0 < \vartheta$.

7.6. Figure 6

Theoretical mean firing rate A_0 as a function of the input potential $h_0 = RI_0$ for an integrate-and-fire neuron with "Gaussian ISI" escape noise compared with the noisy integration model it approximates. **Left:** high noise ($\sigma_u = 1$). **Right:** low noise ($\sigma_u = 0.005$). Thin continuous line, "Gaussian ISI" noise model. Thick dashed line, the theoretical value calculated for diffusion noise using the mean-rate equation (cf. Eq. 7). Parameters: $\tau = 4$ ms, $\eta_0 = 1$, $\vartheta = 0$.

7.7. Figure 7

Linear filters describing the population response to arbitrary small fluctuations. The two components of the filter for an integrate-and-fire neuron with "Gaussian ISI" escape noise are shown. Left, low noise $\sigma_u = 0.005$; right, high noise $\sigma_u = 1$. Solid lines correspond to L_1 and dashed lines to L_2. Note the different vertical scales.

7.8. Figure 8

Integrate-and-fire neurons with "Gaussian ISI" escape noise. Population activities in response to positive and negative alpha-pulses (top, arbitrary scale; rise time 2 ms) at two different noise levels and baseline firing rates. Simulations (thin stepped lines) compared to theoretical responses: the full escape noise model (thick solid curve) integrated numerically using the algorithm in the Appendix, and the linear approximation (dashed). **Left column:** high noise, $\sigma_u = 1$. **Right column:** low noise, $\sigma_u = 0.005$. I_0 was adjusted to compensate for the change in mean activity resulting from the difference in noise levels so that $A_0 \approx 100$ Hz (top row) or ≈ 30 Hz (bottom row). The curves for the 100 Hz low-noise responses are offset for clarity. Adjusting I_0 has a small effect on the amplitude of the peak compared to changing the noise level; cf. Fig. 1(e, right-hand col.) and Fig. 11. In the response calculated with the full model, a discontinuity caused by the $H(u')$ term in the escape rate is seen as a small bump in the bottom left plot. Neuron parameters: $\tau = 4$ ms, $\eta_0 = 1$, $\vartheta = 0$. Simulation parameters: $N = 500,000$ neurons at 100 Hz / $N = 300,000$ neurons at 30 Hz ; time step 0.1 ms (averaged to 0.2 ms in the plots). Input pulse amplitudes were chosen to produce peaks of comparable size, $\Delta A \approx 6$ Hz: at $A_0 = 30\ Hz$, $|\Delta I| = 0.001153$ (low noise) and 0.1562 (high noise); at $A_0 = 100\ Hz$, $|\Delta I| = 0.003888$ (low noise) and 0.06061 (high noise). The integration time step for the full model was 0.05 ms.

7.9. Figure 9

Integrate-and-fire neurons with diffusion noise. Population activities in response to positive and negative alpha-pulses (top curve, arbitrary scale; rise time 2 ms) at two different noise levels and baseline firing rates. Simulations (thin, stepped lines) compared with the theoretical responses (dashed) predicted using the "Gaussian ISI" escape noise model. **Left column:** high noise, $\sigma_u = 1$. **Right column:** low noise, $\sigma_u = 0.005$. As in the previous figure, I_0 was adjusted to compensate for the change in mean activity resulting from the difference in noise levels so that $A_0 \approx 100$ Hz (top row) or ≈ 30 Hz (bottom row). The curves for the 100 Hz low-noise negative-going pulse have been offset for clarity. Neuron parameters: $\tau = 4$ ms, $\eta_0 = 1$, $\vartheta = 0$. Simulation parameters: $N = 500,000$ neurons, time step 0.1 ms (averaged to 0.2 ms). Input amplitudes as in Fig. 8.

7.10. Figure 10

Comparison of the linear approximation with responses from simulations of integrate-and-fire neurons with diffusion noise. Responses to alpha-shaped input pulses(rise time 2 ms) of different amplitudes. Neuron parameters: time constant $\tau = 4$ ms, $\eta_0 = 1$, $\vartheta = 0$. Simulation time step 0.1 ms. (a) High noise, $\sigma_u = 1$, symmetric input pulse sizes $\Delta I = \pm 0.417$. Simulations of $N = 500,000$ neurons, thin stepped lines; full escape noise model, thick solid curve; linear approximation, dashed. (b) As above but with low noise, $\sigma_u = 0.005$; symmetric input pulse sizes $\Delta I = \pm 0.00308$. (c) Peak amplitude of the simulated PSTH as a function of input pulse amplitude at different noise levels. Solid lines, prediction according to Eq. (14) for the "Gaussian ISI" model; symbol shapes, data estimated from simulation results. In the limit $\Delta I \to 0$, the slopes of the simulated responses converge to the theoretical values. An asymmetry is visible: in the diffusion model, the response to negative pulses is often smaller than for positive pulses of the same magnitude. The arrows indicate the points corresponding to plots a and b. Due to a scaling artifact, the lower-noise responses appear to fit the linear approximations better than the higher-noise responses, but in fact all noise levels show the same degree of asymmetry; cf. a and b. Estimated peak amplitudes obtained from the peaks of theoretical curves from the linear model fitted to 60 ms of simulation data from $N = 100,000$ neurons.

7.11. Figure 11

How mean drive level affects the PSTH baseline firing rate (left) and the PSTH peak height (center). The PSTH peak height $|\Delta A|$ was calculated for an α-pulse of amplitude 0.2 nA and risetime 2 ms using the linear filter approximation with the Gaussian-ISI noise model. **Left:** The PSTH baseline A_0 as a function of drive I_0 is shown at three noise levels. The drive level RI_0 is scaled in units of noise amplitude σ_u. The three curves intersect the $A_0 = 30$ Hz level (diamonds) at different drive levels (black triangles). **Center:** PSTH peak height $|\Delta A|$ varies nonlinearly as a function of drive level. The diamonds indicate the peak heights corresponding to the $A_0 = 30$ Hz drive levels highlighted at left. **Right:** Predicted PSTHs at three different noise levels, for the drive levels that give $A_0 = 30$ Hz. (The curve segment that peaks at about $t = 40$ ms is the secondary peak for low noise $\sigma_u = 0.005$; it occurs at about 1 mean period after the initial response.) **Neuron parameters:** time constant $\tau = 4$ ms, $\eta_0 = 1$; threshold $\theta = 0$.

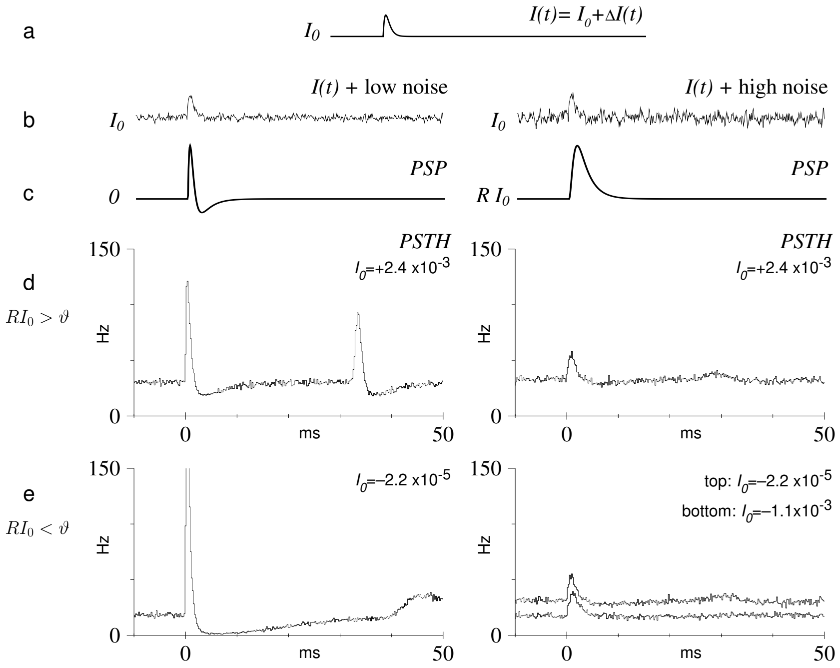

Figure 1.

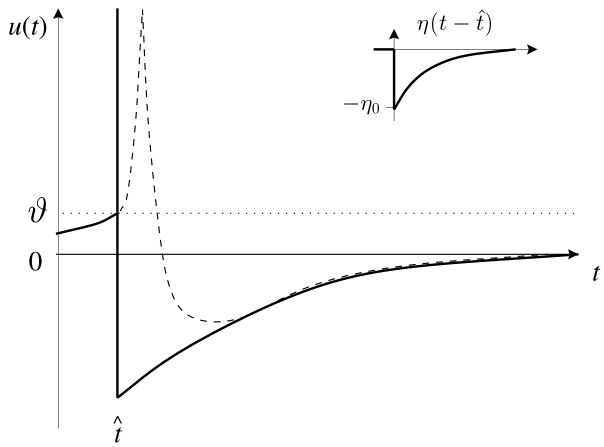

Figure 2.

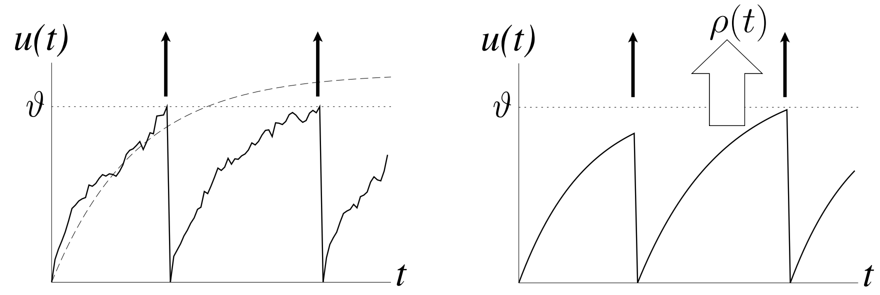

Figure 3.

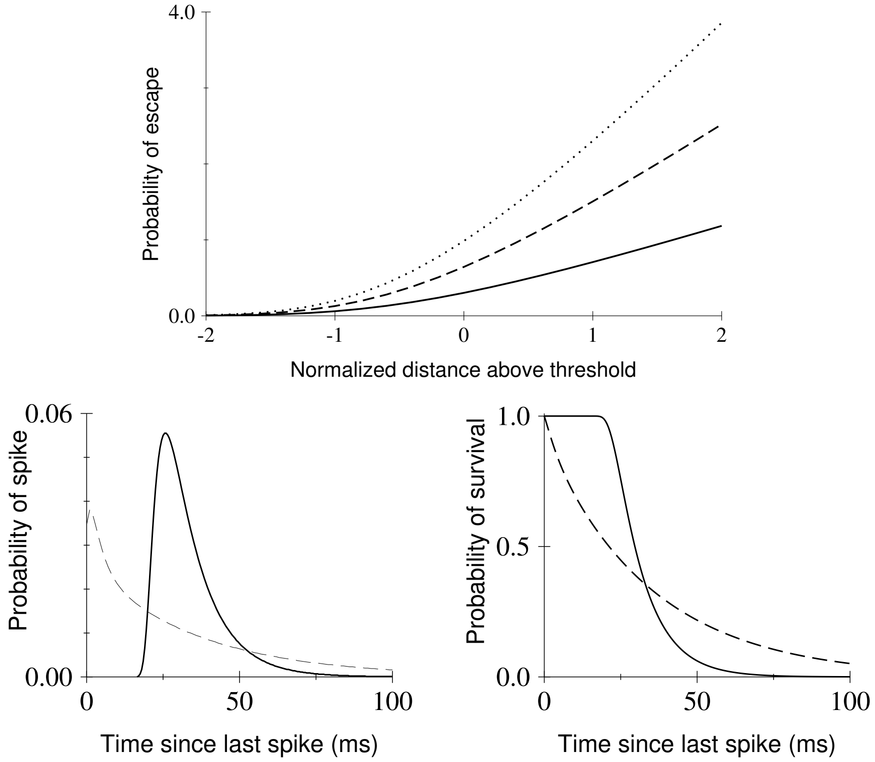

Figure 4.

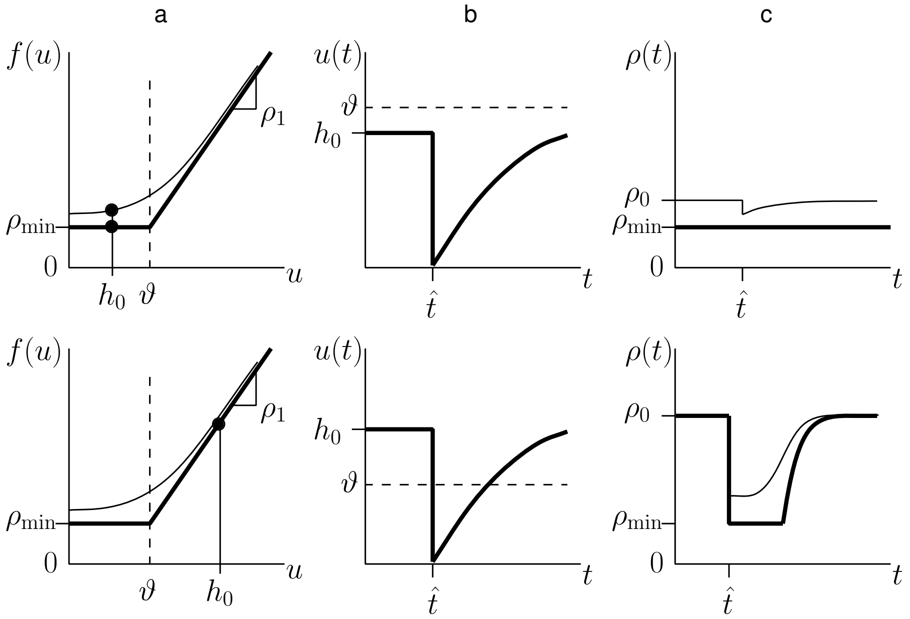

Figure 5.

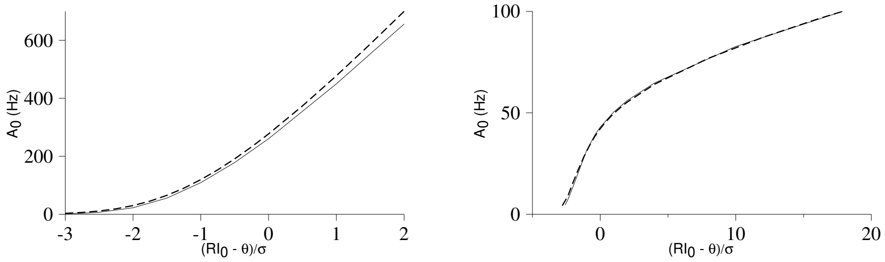

Figure 6.

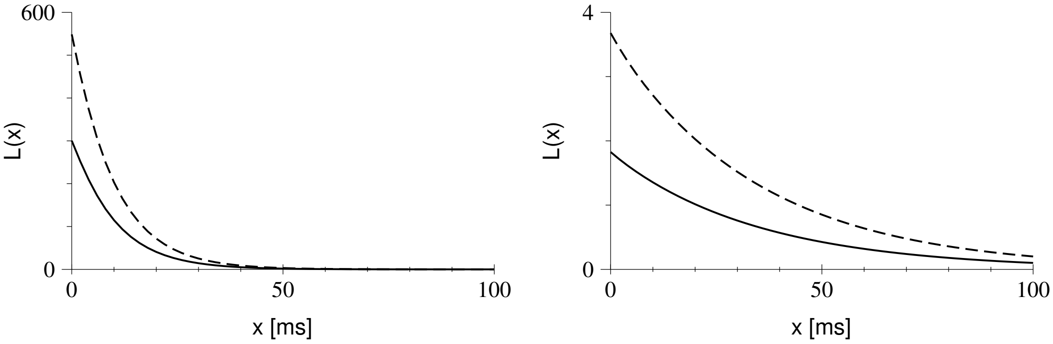

Figure 7.

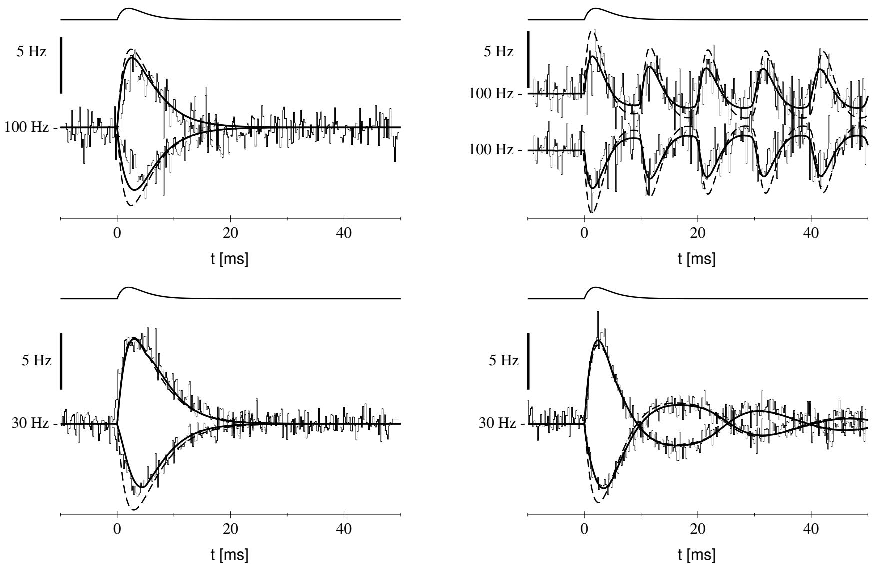

Figure 8.

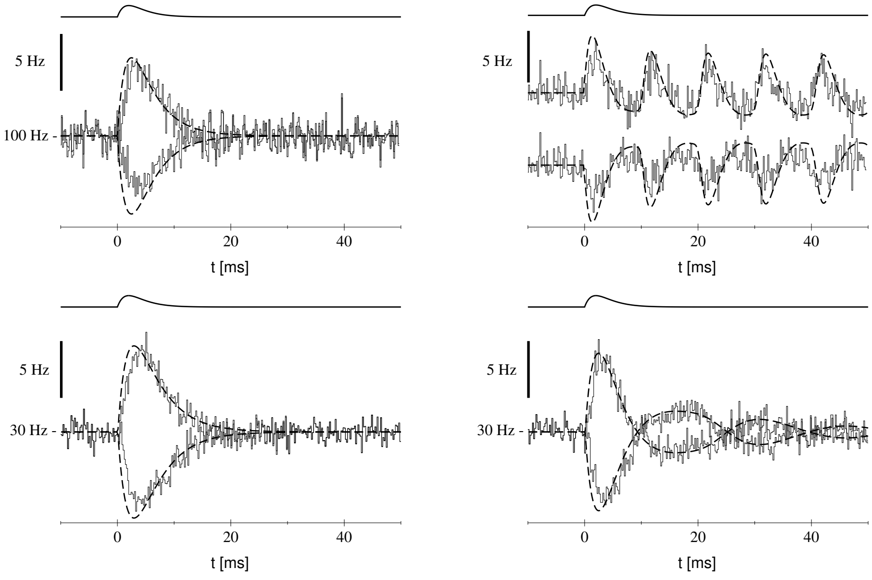

Figure 9.

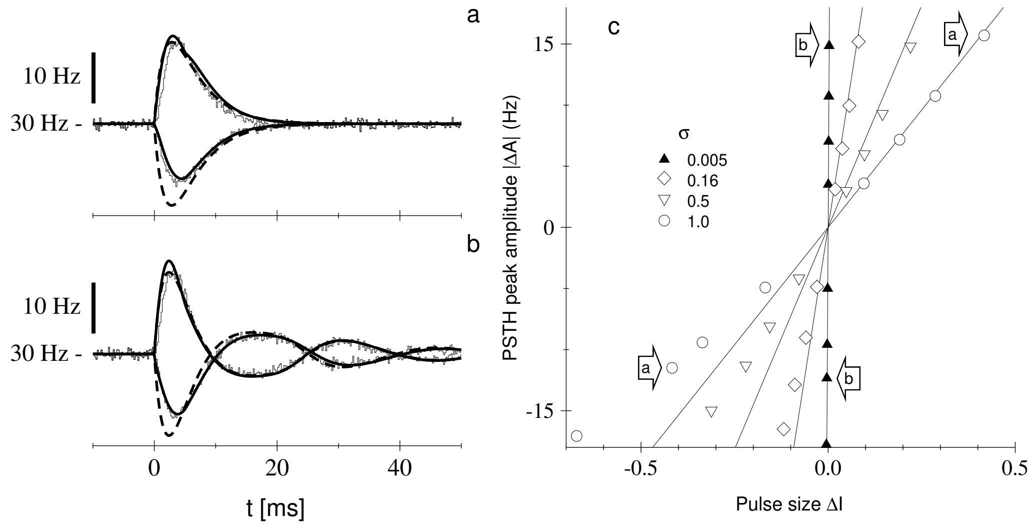

Figure 10.

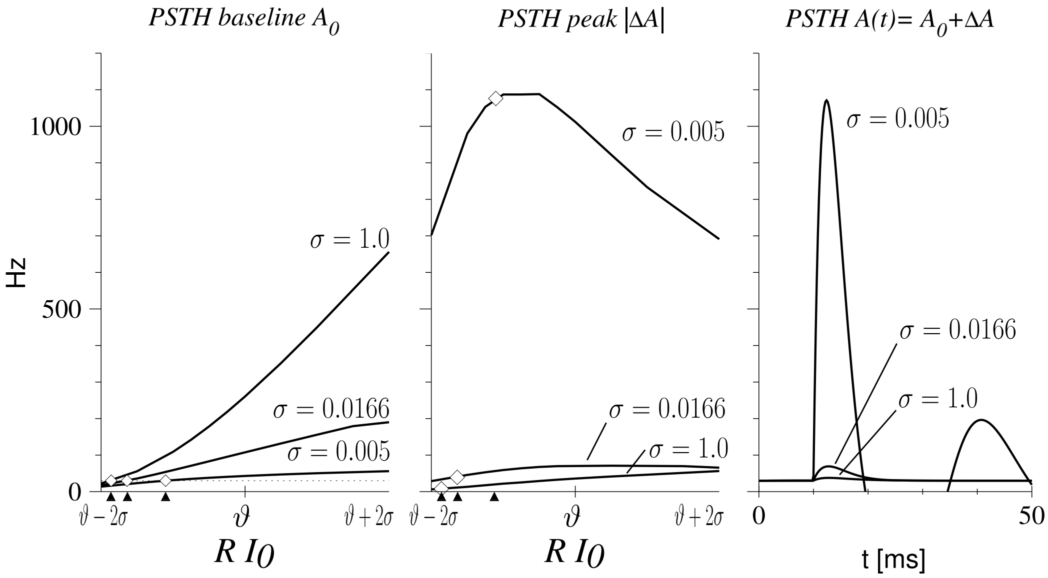

Figure 11.